MIT Libraries | DSpace@MIT

MIT Open Access Articles

Regulated Formation of an Amyloid-like Translational Repressor Governs Gametogenesis

Massachusetts Institute of Technology

Regulated formation of an amyloid-like translational repressor governs gametogenesis

Luke E. Berchowitz[1], **Margaret R. Walker**[1], **Greg Kabachinski**[2], **Thomas M. Carlile**[2], **Wendy V. Gilbert**[2], **Thomas U. Schwartz**[2], and **Angelika Amon**[1,2]

[1] David H. Koch Institute for Integrative Cancer Research and Howard Hughes Medical Institute, Massachusetts Institute of Technology, Cambridge, MA 02139, USA

[2] Department of Biology, Massachusetts Institute of Technology, Cambridge, MA 02139 USA

SUMMARY

Message specific translational control is required for gametogenesis. In yeast, the RNA-binding protein Rim4 mediates translational repression of numerous mRNAs, including the B-type cyclin *CLB3*, which is essential for establishing the meiotic chromosome segregation pattern. Here we show that Rim4 forms amyloid-like aggregates and that it is the amyloid-like form of Rim4 that is the active, translationally repressive form of the protein. Our data further show that Rim4 aggregation is a developmentally regulated process. Starvation induces the conversion of monomeric Rim4 into amyloid-like aggregates thereby activating the protein to bring about repression of translation. At the onset of meiosis II, Rim4 aggregates are abruptly degraded allowing translation to commence. Although amyloids are best known for their role in the etiology of diseases such as Alzheimer's, Parkinson's, and diabetes by forming toxic protein aggregates, our findings show that cells can utilize amyloid-like protein aggregates to function as central regulators of gametogenesis.

Abstract

Contact: Angelika Amon, 77 Massachusetts Ave, 76-561, Cambridge, MA 02139, Phone: 617-258-6559, Fax: 617-258-6558, angelika@mit.edu.

SUPPLEMENTAL INFORMATION

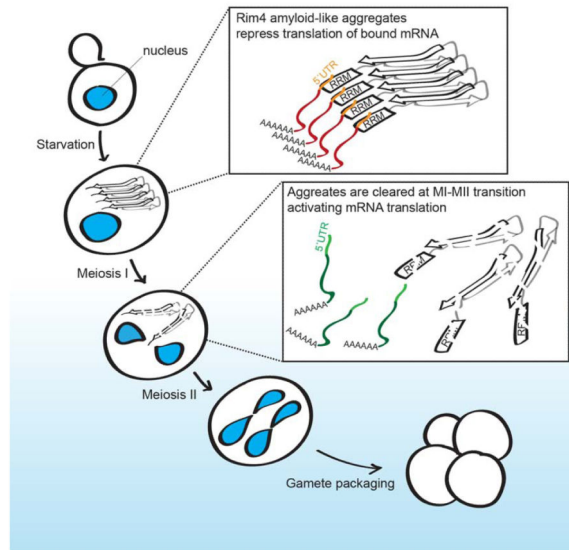Supplemental Information contains Extended Experimental Procedures, six figures, two tables, and six movies.

eTOC Blurb

Amyloid-like aggregation of the RNA-binding protein Rim4 controls gametogenesis by repressing message-specific translation.

INTRODUCTION

Production of haploid gametes from diploid progenitor cells is a hallmark of sexual reproduction. The process is mediated by a specialized cell division, meiosis, where two chromosome divisions, meiosis I and II, follow a single S phase. While meiosis II resembles mitosis in that sister chromatids are separated, meiosis I is unusual in that homologous chromosomes rather than sister chromatids are segregated. Message specific translational control of cyclins is required for progression through the meiotic divisions (reviewed in Kronja and Orr-Weaver, 2011). In budding yeast, translational control of the B-type cyclin *CLB3* is essential for establishing the unusual meiosis I division. *CLB3* mRNA is translationally repressed during meiosis I but is translated during meiosis II (Carlile and Amon, 2008). When *CLB3* is inappropriately expressed during meiosis I, meiosis I chromosome segregation is suppressed. Instead, cells undergo a mitosis-like division illustrating the importance of translational control for gamete formation (Miller et al., 2012).

During meiosis I the RNA-binding protein Rim4 represses the translation of *CLB3* and numerous other mRNAs, the protein products of which are required during the late stages of gametogenesis (Berchowitz et al., 2013). Rim4 binds to the 5´UTR of *CLB3* mRNA and represses translation until the onset of meiosis II. At this stage of meiosis, Rim4 is abruptly degraded. This degradation is controlled by the meiosis-specific protein kinase Ime2 (Berchowitz et al., 2013). These findings made it clear that understanding how Rim4 represses translation is essential to understanding how meiosis and gametogenesis are governed. Here we shed light on this question. We show that Rim4 forms aggregates to repress translation. Rim4 aggregates are SDS-resistant, bind b-isox, and can be pelleted and sedimented from detergent-containing lysate by ultracentrifugation. *In vitro*, Rim4 forms fibrillar structures containing β-sheet. These biochemical properties are indicative of fiber-forming leading us to define Rim4 as "amyloid-like".

Amyloids and amyloid-like aggregates have been implicated in processes such as hormone storage (Maji et al., 2009) and melanin production in mammals (Fowler et al., 2005) and heterokaryon formation in filamentous fungi (Reis et al., 2002). In Drosophila, the Orb2 protein forms oligomers with amyloid-like properties that play a critical role in long-term memory persistence (Majumdar et al., 2012). In mammals, RIP1/RIP3 protein kinases form a heterotypic amyloid complex which is critical for programmed cell necrosis (Li et al., 2012).

While some biological functions have been ascribed to amyloids, these aggregates are predominantly understood in the context of human diseases such as Alzheimer's, Parkinson's, ALS, diabetes, and all known prion diseases (reviewed in (Knowles et al., 2014)). Since their discovery over 150 years ago (Sipe and Cohen, 2000), the main focus of amyloid research has been on understanding the proteins' disease-causing properties. In most if not all diseases associated with amyloids, the aggregates have been proposed to function in a dominant negative manner, sequestering monomeric species into the aggregates causing their depletion within cells. In addition to depleting functional proteins, amyloids are thought to interfere with cellular functions (Thomas et al., 1996), cause cell death (Loo et al., 1993) and, in cases where they are secreted, induce inflammation (Akiyama et al., 2000). Additionally, accumulating evidence suggests that soluble oligomeric amyloid precursors are critical drivers of neurotoxicity and are often described as inherently toxic (Bucciantini et al., 2002; Walsh and Selkoe, 2007). Here, we show that proteins with amyloid-like properties can control gene expression. We demonstrate that the translational repressor Rim4 forms large assemblies with amyloid-like biochemical properties and that it is the aggregated form of Rim4 that is the active, translationally repressive form of the protein. Remarkably, assembly of these structures is developmentally regulated. Upon initiation of sporulation, one of the inducers of the meiotic fate, starvation, induces the switch from monomeric Rim4 into amyloid-like Rim4 rendering the protein competent to repress *CLB3* translation. At the onset of meiosis II translational repression of *CLB3* is lifted through the degradation of Rim4 aggregates. Our results demonstrate that regulated formation of amyloid-like aggregates establishes and upholds gametogenesis.

RESULTS

Rim4 is efficiently precipitated from meiotic lysate by b-isox

To begin to understand how Rim4 represses translation we used computational approaches to identify potential functional domains within the protein. Rim4 contains three N-terminal RNA-recognition motifs (RRMs) that are required for RNA binding and translational repression (Berchowitz et al., 2013). The protein also contains a C-terminal low-complexity (LC) region (**Figure 1A**), harbors two poly-N stretches and a computationally predicted prion domain (Alberti et al., 2009; Soushko and Mitchell, 2000). Several RNA-binding proteins containing LC sequences have the ability to form amyloid-like fibrous aggregates. Aggregation of these proteins is important for the formation of nonmembrane-bound intracellular compartments such as RNA granules (Kato et al., 2012) which have been shown to function in translational control (Kronja and Orr-Weaver, 2011).

Many fiber-forming RNA-binding proteins can be precipitated from aqueous solution or cell extracts by binding to the compound biotinylated isoxazole (b-isox) via their LC sequences (Kato et al., 2012). To determine whether Rim4 exhibits this property and thus shares biochemical similarity with other fiber-forming RNA-binding proteins, we asked whether Rim4 binds to b-isox. In order to obtain a uniform population of cells in which Rim4 inhibits translation, we induced cells lacking the transcription factor Ndt80 to undergo sporulation. Cells lacking Ndt80 progress through the early stages of the meiotic cell cycle efficiently but arrest in G2 prior to meiosis I entry (Xu et al., 1995). In this cell cycle stage Rim4 is active and translation of *CLB3* is inhibited (Berchowitz et al., 2013). We found that b-isox efficiently precipitated Rim4 from lysates prepared from cells lacking Ndt80 (**Figure 1B**).

To determine more precisely when during meiosis b-isox was able to precipitate Rim4 we examined cells induced to progress through a synchronous meiosis using the *NDT80* block-release system. In this system, *NDT80* expression is driven from the *GAL1-10* promoter (*pGAL-NDT80*) that in turn is controlled by an estradiol-regulatable Gal4-ER fusion (*GAL4.ER*). *pGAL-NDT80* cells will arrest in meiotic G2 in sporulation medium lacking estradiol but will progress synchronously through the meiotic divisions upon estradiol addition (Benjamin et al., 2003; Carlile and Amon, 2008). Rim4 was efficiently precipitated by b-isox for 2 hours following the release from the G2 block, when cells were in meiosis I (**Figures 1C, D**). As shown previously (Berchowitz et al., 2013), when cells enter meiosis II, Rim4 was degraded (**Figures 1C, D**).

To assess the specificity of b-isox we used quantitative mass spectrometry to query the yeast proteome for meiotic b-isox binding proteins. We released cells from the *NDT80* block and collected samples spanning the two meiotic divisions (**Figure S1**). B-isox was remarkably selective. Rim4 was among the most enriched proteins during meiosis I (1 hour after release from the G2 block; **Figures 1E, F**) and only four other proteins, among them the prion Sup35, exhibited significant enrichment (**Table S1**; **Figure 1E**). We conclude that Rim4, like prions and other proteins with amyloid-like properties, binds to b-isox and does so during the stages of meiosis when the protein actively inhibits *CLB3* translation.

Rim4 forms amyloid-like aggregates *in vitro*

Yeast prions and other amyloidogenic proteins such as Huntingtin form amyloid aggregates via regions within the protein rich in N and Q residues (DePace et al., 1998; Scherzinger et al., 1997). Given that Sup35 and Rim4 were efficiently precipitated by b-isox and that Rim4 contains poly-N stretches we next asked whether Rim4, like Sup35, forms amyloid-like aggregates *in vitro*. We generated highly purified recombinant Rim4 harboring minimal nucleic acid contamination (**Figures S2A-C**) and analyzed concentrated protein by transmission electron microscopy (TEM). At a concentration of 40 mg/ml, Rim4 formed fibrillar helical structures with a fixed width of ~15 nm and length up to 15 μm visible by both negative stain and cryo TEM (**Figure 2A**). The ability to form fibers depended on the protein's C-terminal LC sequences. A mutant derivative lacking the C-terminal 294 amino acids but leaving the 3 RRMs intact (Rim4 294C) did not form long helical fibers (**Figure 2B**). Because Rim4 is an RNA-binding protein (Berchowitz et al., 2013), we examined the effects of RNA on Rim4 fiber formation. Incubation of monomeric Rim4 with a bona fide

RNA target, the *CLB3* 5′UTR, or total RNA did not induce fiber formation as assessed by TEM (**Figure S2D**). Furthermore, RNase treatment of pre-formed fibers did not result in fiber disassembly (**Figure S2E**). These results indicate that fiber formation *in vitro* can occur in the absence of RNA.

Biochemical analyses further demonstrated that Rim4 fibers are composed of β-sheets, a hallmark of amyloid. Circular dichroism (CD) spectrum analysis of fibrous Rim4 revealed a minimum at 218 nm (**Figure S2F**), which is characteristic of structures rich in β-sheet. In contrast, the CD spectrum of Rim4 294C was predominated by α-helical signature (**Figure S2F**). Furthermore, Rim4 but not Histone H1 bound to Thioflavin T (ThT), a dye that stains the β-sheet rich structures of amyloid and not monomers (Nilsson, 2004) (**Figure 2C**). Rim4 lacking the C-terminal LC sequences also bound Thioflavin T but with reduced affinity compared to full-length protein (**Figure 2C**). We speculate that the N-terminal disordered sequence (**Figure 1A**) mediates the production of some β-sheet structures in the truncated protein. In concordance with these results we observed that Rim4 is recognized by an α-amyloid fibril antibody (α-amyloid fibrils OC, Millipore) (**Figure 2D**). Rim4 294C is recognized to a much lesser extent and Histone H1 not at all. We note that unlike other LC-sequence containing proteins (Kato et al., 2012), Rim4 did not form hydrogels, even when incubated at 4°C for months at high conce ntrations. Nevertheless, our analyses demonstrate that recombinant Rim4 forms aggregates with several morphological and biochemical properties of amyloid in the absence of other proteins or nucleic acids and that the C-terminal LC sequences are critical for fiber formation.

Evidence that Rim4 forms aggregates *in vivo*

Amyloid-like aggregates can form stable structures *in vivo* as judged by fluorescence recovery after photobleaching (FRAP)(Kayatekin et al., 2014). For example, when the amyloidogenic Huntingtin protein harboring a greatly expanded poly-Q stretch (Htt103Q) is expressed in yeast, aggregated foci display very little signal recovery after photobleaching whereas non-aggregating Huntingtin proteins exhibit rapid signal recovery (Kayatekin et al., 2014). To determine whether Rim4 forms aggregates *in vivo* we analyzed the FRAP kinetics of wild-type and aggregate-defective Rim4 that lacks the C-terminal 204 amino acids (Rim4 204C) in sporulating cells (**Figures 3A, B**). After photobleaching, wild-type Rim4 showed minimal recovery while the Rim4 204C signal recovered with similar kinetics as the soluble cytoplasmic enzyme Pgk1. This result demonstrates that Rim4 structures within the cell are largely static. This rigidity depends on Rim4's C–terminal 204 amino acids.

The localization pattern of Rim4 is also consistent with the protein forming aggregates in cells during stages of meiosis when the protein inhibits translation. In meiotic G2-arrested cells, Rim4 protein levels were similar between wild-type and Rim4 204C as judged by signal intensity within a fixed area of the cell (**Figure 3C, D**). However, whereas the Rim4 204C signal was uniformly distributed throughout the cytoplasm, wild-type Rim4 appeared more focal, leading to a more granular staining pattern (**Figure 3C**). This was most evident when we analyzed heterogeneity in pixel intensity by comparing the standard deviations of the mean pixel signal intensity within a defined area of cytoplasm. The

standard deviation was significantly higher for wild-type Rim4 than the aggregate-defective Rim4 204C mutant protein (**Figure 3E**).

To determine whether the C-terminal LC sequences of Rim4 affect Rim4 clearance we compared protein levels of wild-type Rim4 and the Rim4 204C mutant in live cells undergoing meiosis. To ensure that the Rim4 mutant protein did not affect meiotic progression we conducted the experiment in diploid cells that carried one wild-type copy of *RIM4* and either one EGFP-tagged wild-type *RIM4* or *rim4 204C* allele. Rim4 accumulated during premeiotic S phase and persisted throughout meiosis I at which point Rim4 was abruptly degraded (**Figures 3F, S3A, S3B, Movies S1-4**). Surprisingly, Rim4 204C was not cleared from cells efficiently compared to Rim4-EGFP (**Figures 3F, S3C, Movies S5-S6**). The mutant protein persisted in cells well beyond exit from meiosis I. This result indicates that the C-terminal 204 amino acids are important for Rim4 aggregation *in vivo* and contain elements necessary for proper Rim4 clearance at the onset of meiosis II.

Rim4 forms SDS-resistant aggregates during meiosis

To further examine whether Rim4 indeed forms amyloid-like aggregates *in vivo*, we employed semi-denaturing detergent agarose gel electrophoresis (SDD-AGE). Amyloid (as opposed to amorphous or globular) aggregates are SDS-resistant and SDD-AGE allows for the resolution of these structures (Alberti et al., 2009). Rim4 formed SDS-resistant aggregates in cells progressing through meiosis in a synchronous manner (**Figure 4A**). Previously described fiber-forming (hydrogelling) RNA-binding proteins do not form SDS-resistant structures (Kato et al., 2012). Thus Rim4 forms different structures from the fiberizing RNA-binding proteins that form hydrogels. However, we cannot rule out that Rim4 aggregates adopt a higher-order static hydrogel state within the cell.

Rim4 aggregates formed as soon as the protein was produced during premeiotic S phase and persisted throughout meiosis I. During meiosis II, SDS-resistant aggregates were no longer detected. We note that while SDS-resistant Rim4 aggregates were absent during meiosis II we did detect Rim4 protein in extracts prepared by boiling cells in SDS-PAGE buffer (compare Figures 4A and B). We can envision two not mutually exclusive explanations for this observation. First, incomplete synchrony of cells progressing through meiosis could be responsible. The Rim4 protein detected in meiosis II time points by SDS-PAGE could originate from cells that either did not enter sporulation or arrest at some point in meiosis prior to Rim4 aggregate formation. Second, Rim4 aggregates could be disassembled in meiosis II before they are degraded. We note that monomeric Rim4 is not detected in SDD-AGE in these late meiotic time points but previous studies indicated that SDD-AGE does not reliably detect monomeric proteins (Halfmann et al., 2012). It is also possible that monomeric Rim4 is unstable (indeed the protein is degraded during meiosis II) and hence degraded during the lengthy SDD-AGE extract preparation procedure. Irrespective of whether or not Rim4 aggregates are disassembled prior to their degradation, the presence of amyloid-like Rim4 aggregates in cells correlated with Rim4-mediated translational repression. Clb3 protein levels accumulated as Rim4 aggregates were degraded (**Figures 4A-C**). This finding raises the interesting possibility that it is the amyloid-like form of Rim4 that mediates translational repression.

To further explore whether translational repression of *CLB3* correlates with Rim4 aggregation, we utilized a construct where *CLB3* expression can be induced at will from the *GAL1-10* promoter (driven by a Gal4-ER fusion) but that preserves translational control of *CLB3* (henceforth *pGAL-5´UTR$_{CLB3}$-CLB3*). If Rim4 amyloid-like aggregation is important for its function, *CLB3* translational repression should correlate with aggregate formation. To test this prediction, we assessed when during early stages of sporulation *CLB3* becomes translationally repressed. We induced expression of *CLB3* from the *pGAL-5´UTR$_{CLB3}$-CLB3* fusion at various times after the induction of sporulation in cells lacking *NDT80* that progressed through sporulation in a synchronous manner (for a detailed description of the experimental setup see **Figure S4A**). *CLB3* translation occurred efficiently within the first 2 hours after induction of sporulation. By three hours however, when cells had entered pre-meiotic S phase, *CLB3* translation was repressed as judged by the lack of Clb3 protein despite ample induction of *CLB3* expression (**Figures 4D, S4B**). Translational repression persisted until the end of the experiment when cells had arrested in G2 due to the lack of *NDT80*. Loss of *CLB3* translation correlated remarkably well with the formation of SDS-resistant Rim4 aggregates (**Figures 4E, F**). Taken together these data indicate that cells generate RNA-binding amyloid-like aggregates of Rim4 to mediate translational control of gene expression *in vivo*.

The LC sequences of Rim4 mediate formation of amyloid-like aggregates and translational repression

To determine whether the formation of amyloid-like Rim4 aggregates was required for translational repression of *CLB3* mRNA we first identified the region within Rim4 responsible for aggregation *in vivo*. Two recent reports have shown that RNA stimulates formation of amyloid-like fibers of the RNA-binding protein FUS by increasing local concentration and thus nucleating assembly (Kato et al., 2012; Schwartz et al., 2013). Does Rim4's RNA-binding property mediate amyloid-like aggregation? To address this question we analyzed SDS-resistant aggregate formation in a *rim4-F139L* mutant. The *rim4-F139L* mutant encodes a protein in which a critical phenylalanine residue in the first RRM domain is mutated to leucine (Soushko and Mitchell, 2000). The RRM mutant formed amyloid-like aggregates equally well as wild type Rim4 *in vitro* and *in vivo*. Recombinant Rim4-F139L purified and concentrated to 27 mg/ml forms fibers *in vitro* (**Figure 5A**) and SDS-resistant aggregates *in vivo* (**Figure 5B**). We conclude that RNA-binding is not a prerequisite for aggregation *in vitro* and *in vivo*.

The LC sequences of Rim4 are a prime candidate for mediating the formation of Rim4 amyloid-like aggregates. Indeed, deleting the C-terminal 271 amino acids that comprise the LC sequences (**Figure 5C**) abrogated the formation of SDS-resistant aggregates *in vivo* (**Figure 4A**). As an alternative method to assess the importance of the C-terminal region of Rim4 in aggregate formation, we employed differential centrifugation. The unusual detergent-insolubility of amyloid-like aggregates allows for the sedimentation of these particles by ultracentrifugation from native lysates in the presence of detergent (Sondheimer and Lindquist, 2000). We assayed the sedimentation properties of *RIM4-3V5* as well as two *rim4* mutants lacking either most (*rim4 271C-3V5*) or a portion of the LC sequences (*rim4 138C-3V5)*. We observed full-length Rim4 protein predominantly in the pellet

fraction while the aggregate-defective mutants remained in the supernatant (**Figure 5D**). We conclude that the C-terminal LC sequences of Rim4 are required for aggregation of the protein *in vivo*.

If amyloid-like aggregates are required for translational control, then abrogation of Rim4 aggregation should result in loss of *CLB3* translational repression. To test this prediction, we examined the consequences of deleting increasingly larger portions of the C-terminal LC sequences of Rim4 on aggregate formation and *CLB3* translation. We arrested cells in meiotic G2 by deleting *NDT80* and then induced expression of *CLB3* from the aforementioned *pGAL-5´UTR$_{CLB3}$-CLB3* fusion. In cells expressing full-length Rim4 *CLB3* translation was inhibited (**Figures 5C, E**). However, deleting as few as the terminal 66 amino acids led to *CLB3* translation in G2-arrested cells (**Figures 5C, E**). Larger deletions further increased translation efficiency.

Expressing Clb3 in G2-arrested cells had consequences. Upon *CLB3* induction, *rim4* aggregation-defective cells inappropriately formed meiosis I spindles in the G2 arrest, causing the appearance of cells with characteristics of both the *ndt80?* G2 arrest and meiosis I. Cells harbored separated spindle pole bodies (a meiosis I characteristic) and the synaptonemal complex protein Zip1 accumulated in the nucleus (a *ndt80?* arrest characteristic; **Figure S5**). Importantly, Rim4 truncations that failed to inhibit *CLB3* translation also failed to form SDS-resistant aggregates (**Figure 5F**). These findings show that aggregation and inhibition of translation are mediated by Rim4's LC domain.

Because the larger C-terminal deletions led to an approximately 50% decrease in Rim4 protein levels (**Figure 5E**) we also examined the effects of reducing the levels of full-length Rim4 by a similar degree. A *RIM4/rim4?* heterozygous strain produces approximately equivalent amounts of Rim4 as a strain carrying two copies of a *RIM4* allele producing a truncation lacking the C-terminal 138 aa (*rim4 138C-3V5*) but translational repression was largely unaffected compared to *rim4 138C-3V5* cells (**Figures 5E, S5**). We conclude that the loss of translational repression observed in *rim4* aggregation-defective mutants is not due to decreased protein levels. Rather, we propose that it is caused by an inability to form high molecular weight aggregates.

Rim4 amyloid-like aggregates sequester *CLB3* mRNA

Aggregation-defective *rim4* mutants could abrogate translational control because they fail to bind RNA, repress translation, or both. To determine whether amyloid-like aggregation of Rim4 is important for RNA-binding, we performed extract-binding studies. We transcribed the *CLB3* 5´UTR along with two controls *in vitro*: the *CLB3* 5´UTR with a 25 nucleotide (nt) deletion and the 248 nt *CLB1* 5´UTR. These controls bind Rim4 with decreased affinity compared to the *CLB3* 5´UTR (Berchowitz et al., 2013). We coupled these RNAs via a biotin group to streptavidin beads and assayed the ability of the RNA to pull down Rim4 or an aggregation-defective mutant (Rim4 138C) from extracts prepared from G2-arrested cells, when Rim4 inhibits translation. We found that the RNA-binding activity of the aggregation-defective Rim4 was reduced by 50% (**Figures 6A, B**). These results indicate that the ability of Rim4 to aggregate is important for its ability to bind RNA. However, the

2-fold reduction in RNA-binding exhibited by Rim4 138C is unlikely to explain the greater than 20-fold increase in translational efficiency of the mutant. We propose that while amyloid-like aggregation is required for efficient RNA-binding, Rim4 aggregates participate in translational control beyond their role in RNA-binding.

Having determined that Rim4 aggregation plays only a minor role in RNA binding we next tested the possibility that the Rim4 amyloid-like aggregates mediate repression of *CLB3* mRNA translation. If Rim4 aggregates repress translation, *CLB3* mRNA should cofractionate with Rim4 aggregates but not Rim4 monomers or oligomers. Furthermore, in *rim4* mutants that fail to form amyloid-like aggregates, *CLB3* mRNA ought to fractionate with translating ribosomes. To test these predictions we fractionated lysates from *RIM4-3V5* and *rim4 138C-3V5* cells arrested in meiotic G2 (when *CLB3* is translationally repressed) in 10-50% sucrose gradients. This analysis showed that both Rim4 and *CLB3* mRNA were present in the heaviest fractions of the gradient (**Figures 6C, D**). In contrast, Rim4 138C was predominantly present in the light fractions of the gradient and did not co-fractionate with *CLB3* mRNA. Instead, *CLB3* mRNA was found enriched in heavy fractions of the gradient likely due to its association with translating ribosomes. Our analyses of wild-type and Rim4 mutant proteins in SDD-AGE as well as sedimentation and sucrose gradients indicate that it is the aggregated form of Rim4 that mediates translational repression.

Gametogenesis signals regulate Rim4 amyloid formation

Our results show that Rim4 forms amyloid-like aggregates during meiosis I to inhibit *CLB3* translation. Is this process regulated and if so which aspect of the regulatory network that induces sporulation controls the aggregation of Rim4? Two signals trigger gametogenesis in budding yeast: mating type and starvation (reviewed in (van Werven and Amon, 2011)). Only cells of the MATa/α mating type can undergo sporulation and they do so only when they are starved, that is when they are deprived of nitrogen and a fermentable carbon source.

To determine whether formation of Rim4 amyloid-like aggregates is regulated by these gametogenesis-inducing signals we asked whether ectopically expressed Rim4 aggregates in haploid cells grown in nutrient-rich medium supplied with ample nitrogen and glucose (YEPD medium). *RIM4* expressed under the control of the copper-inducible *CUP1* promoter readily produced Rim4 protein in YEPD medium but the protein did not form amyloid-like aggregates as judged by the lack of SDS-resistant Rim4 particles (**Figures 7A, B, S6A**). Accordingly, *CLB3* was translated effectively (**Figure 7A**). In contrast, starvation caused Rim4 to form SDS-resistant aggregates. We starved haploid cells for 4 hours in sporulation medium and then induced Rim4 expression. Rim4 readily aggregated under these growth conditions and inhibited translation of *CLB3* (**Figures 7A, B**). These results indicate that the gametogenesis-inducing starvation signal causes the formation of Rim4 amyloid-like aggregates. Our data further demonstrate that monomeric Rim4 cannot repress *CLB3* translation.

To directly test that starvation induces Rim4 aggregation we expressed Rim4 in haploid cells grown in nutrient rich conditions (BYTA) when the protein is largely in its monomeric form. We then repressed *RIM4* expression and simultaneously starved cells by transferring them into sporulation medium (**Figures 7C, S6B**). Within 30 min of inducing starvation,

monomeric Rim4 converted into amyloid-like aggregates (**Figures 7C, S6C**). We conclude that aggregation of Rim4 is a regulated process. Monomeric Rim4 assembly into amyloid-like aggregates is induced by starvation signals to convert the protein into an amyloid-like translational repressor.

DAZL forms SDS-resistant aggregates in vivo

Although budding yeast harbors many proteins with RRM domains and a prion domain, only Rim4 is sporulation-specific. In humans, there are only four such gametogenesis-specific proteins. They are *DAZ1-4* (King et al., 2012). These four proteins exist as a cluster on the Y-chromosome- a region of the Y that is often found deleted in infertile men with a condition called azoospermia (Reijo et al., 1995). While *DAZ* exists only in humans and old world monkeys, one of its autosomal homologs *DAZL* (*DAZ*-like) is found from fish to humans (Haag, 2001). Like Rim4, DAZL functions in the regulation of translation (Collier et al., 2005) and is essential for gametogenesis in many organisms, including mice (Ruggiu et al., 1997). We found that mouse DAZL forms SDS-resistant aggregates in cells undergoing gametogenesis (testes), but not in brain, intestine and liver, **Figures 7D, E**). We propose that DAZL (and possibly DAZ) functions to regulate translation of gametogenesis-specific RNAs in a manner similar to Rim4 and suggest that amyloid-like aggregation of RNA-binding proteins is an evolutionarily conserved feature of gametogenesis.

DISCUSSION

Here we show that amyloid-like aggregates, generally considered to be inactive and often toxic, play a central role in creating the cell division essential for gamete formation and hence sexual reproduction. Rim4 represses the translation of *CLB3* during meiosis I which is critical to establish the meiosis I chromosome segregation pattern. Rim4 does so by forming amyloid-like aggregates. Importantly, formation of these structures is regulated. Starvation, one of the signals that triggers gamete development, induces the conversion of monomeric Rim4 into aggregated Rim4. Thus starvation not only initiates gametogenesis but also sets up the mechanism that brings about the meiotic chromosome segregation pattern much later during gamete formation.

Rim4 aggregation is a regulated process

Several lines of evidence demonstrate that Rim4 forms large amyloid-like aggregates *in vivo*. The protein is immobile and found in granular structures within cells, forms SDS-resistant aggregates when isolated from cell extracts, can be sedimented and fractionated from undenatured detergent-containing lysates, and can be quantitatively precipitated from cell extracts using b-isox. The protein's *in vitro* properties: Thioflavin T binding, fiber formation, CD spectrum, and reactivity with an anti-amyloid antibody further support the idea that Rim4 has amyloid-like properties.

Our data lead to the conclusion that aggregation of Rim4 is a regulated process. When we express Rim4 in cells grown in nutrient-rich conditions the protein is monomeric, but upon transfer into sporulation-inducing conditions the protein quickly converts into the aggregated form. During normal progression through sporulation we do not observe this

conversion. This is not surprising because *RIM4* is only induced during premeiotic DNA replication, after cells have been transferred into starvation-inducing medium. Thus, Rim4 is immediately assembled into amyloid-like aggregates upon its expression. We do not yet know how starvation induces Rim4 assembly. Down-regulation of the RAS and TOR pathways is likely to play a central role in the process. Once we understand how amyloid assembly is controlled *in vivo* we can begin to think about strategies to reverse the process. These could very well in time result in the identification of anti-amyloid treatments.

Once Rim4 aggregates into amyloid-like structures and binds to target RNAs it inhibits translation until the completion of meiosis I (**Figure 7F**). At the onset of meiosis II Rim4 aggregates are degraded by an unknown mechanism allowing translation to commence. Our studies suggest that the C-terminal LC sequences are critical for this degradation. This finding raises the interesting possibility that Rim4 must be in the amyloid-like form to be cleared from cells. This would imply that autophagy degrades Rim4 structures at the end of meiosis I. However, we have not detected Rim4-EGFP in the vacuole at the time of its degradation at the onset of meiosis II, arguing against autophagy-mediated clearance of Rim4. Rim4 could be eliminated by proteasomal degradation, but such a mechanism would likely require prior aggregate disassembly. Our previous studies have implicated Ime2-mediated phosphorylation in triggering Rim4 degradation (Berchowitz et al., 2013). Perhaps Ime2 phosphorylation triggers Rim4 disassembly and degradation by the proteasome. Amyloids and amyloid-like aggregates are usually stable and long-lived. Understanding how they are cleared from cells at the appropriate developmental transition leaving Rim4 target RNAs intact ready to be translated will be critically important.

Mechanisms of translational repression by Rim4

Why must Rim4 assemble into amyloid-like particles to repress translation? An aggregate-based apparatus rather than a mechanism involving monomer binding could be used to localize the translationally inhibited mRNA to certain sites within the cell where the protein products are eventually needed. This is unlikely to be the case for Rim4. The protein does not show any localization preference within the cytoplasm (Berchowitz et al., 2013). The amyloid-like state could allow for heterotypic interactions with other proteins with amyloid-like properties that are involved in translational repression. Amyloids have the ability to influence cross-seeding of other amyloidogenic proteins (Derkatch and Liebman, 2007). A computational survey in budding yeast identified 179 proteins harboring prion domains many of which exhibit canonical properties of amyloid-forming proteins (Alberti et al., 2009). Many of these proteins are involved in RNA processing and translational control. Cross-seeding between proteins with amyloid-like properties could offer a mechanism for the assembly of translationally repressive cytoplasmic structures similar to P-bodies (Decker et al., 2007).

Translational control mediated by amyloid-like aggregates could be a universal property of gametogenesis

A significant proportion of RRM-containing proteins also contain a prion domain and/or LC-sequences. This raises the interesting possibility that regulation of RNA functions by amyloid-like aggregates is a frequently used mechanism of controlling gene expression

(Kato et al., 2012; King et al., 2012). In budding yeast, about 1% of genes encode proteins bearing RRM domains (52 genes) and about 3% of genes encode proteins containing a prion domain (179 genes) (Alberti et al., 2009). 13 genes encode proteins with both an RRM and prion domain. This is approximately 10-fold higher than is expected to occur at random. A similar situation exists in humans. The coexistence of RRM and prion domains within the same protein is 13-fold higher than what would be expected to occur by chance (King et al., 2012). This association has led to the proposal that multimerization via prion domains or LC sequences is necessary for the function of many RNA-binding proteins. Indeed, several RNA-binding proteins containing a prion domain have well-characterized roles in translational control such as Ccr4, Pat1, TIF4632 (eIF4G), and Whi3. Understanding under which circumstances an amyloid-like structure can promote or repress translation will provide critical insights into the pathogenesis of amyloids.

Remarkably, both yeast and mouse contain an RNA-binding protein, Rim4 and DAZL, respectively, that functions in translation and forms SDS-resistant aggregates during gametogenesis. This finding raises the possibility that DAZL forms amyloid-like aggregates to regulate translation. Additionally, it leads to the speculation that gametogenic processes as diverse as spore formation in yeast and sperm production in mammals are fundamentally related and rely on an ancient process that involves the formation of large amyloid-like aggregates.

EXPERIMENTAL PROCEDURES

Sporulation conditions

Strains were grown to saturation in YPD, diluted in BYTA (1% yeast extract, 2% tryptone, 1% potassium acetate, 50 mM potassium pthalate) to $OD_{600} = 0.25$ and grown overnight. Cells were resuspended in sporulation medium (0.3% potassium acetate [pH 7.0], 0.02% raffinose) to $OD_{600} = 1.8$ and sporulated with vigorous shaking at 30°C. *pGAL-NDT80, GAL4.ER* strains were released from the arrest by the addition of 1 μM β-estradiol at 6 hr. In *ndt80?* strains, expression of *pGAL-5′UTR$_{CLB3}$CLB3-3HA* was induced with 1 μM β-estradiol at the indicated times.

Transmission electron microscopy

For negative staining, 10 μl of protein solution was applied to a TEM grid (Electron Microscopy Sciences), washed with distilled water, and stained with several drops of 1% or 2% (w/v) aqueous uranyl acetate. Excess stain was removed and the grids air-dried. TEM images were obtained at 80 kV on an FEI Technai Spirit TEM. For cryo-TEM, 10 μl of protein solution was applied to a TEM grid, washed with distilled water and plunged into cooled liquid ethane. TEM images were obtained at 120 kV on a JEOL 2100 FEG TEM.

Semi-denaturing detergent agarose gel electrophoresis (SDD-AGE)

2 ml samples of sporulating culture were harvested by centrifugation and snap frozen in liquid nitrogen. Cell pellets were resuspended in lysis buffer (100 mM Tris/HCl pH 8.0, 20 mM NaCl, 2 mM MgCl$_2$, 50 mM β-mercaptoethanol, 1% Triton-X, 2x Halt protease inhibitors (Thermo)) and broken using a Fast Prep (MP bio) and zirconia beads (BioSpec).

The lysates were clarified twice by centrifugation at 2,500 rcf for 5 min (4°C). Loadin g buffer (final concentration 0.5x TAE, 5% glycerol, 2% SDS, bromophenol blue) was added to lysates which were then incubated for 10 min at room temperature. Following incubation, samples were separated on a 1.7% agarose gel for 16 hours at 29 V at 4°C using 1x TAE supplemented with 0.1% SDS as the running buffer. The gel was blotted to nitrocellulose by downward capillary transfer in 1X TBS and processed by the immunoblot procedure outlined in supplementary methods.

Supplementary Material

Refer to Web version on PubMed Central for supplementary material.

ACKNOWLEDGEMENTS

REFERENCES

Akiyama H, Barger S, Barnum S, Bradt B, Bauer J, Cole GM, Cooper NR, Eikelenboom ME, Emmerling M, Fiebich BL, et al. Inflammation and Alzheimer's disease. Neurobiol. Aging. 2000; 21:383–421. [PubMed: 10858586]

Alberti S, Halfmann R, King O, Kapila A, Lindquist S. A systematic survey identifies prions and illuminates sequence features of prionogenic proteins. Cell. 2009; 137:146–158. [PubMed: 19345193]

Benjamin KR, Zhang C, Shokat KM, Herskowitz I. Control of landmark events in meiosis by the CDK Cdc28 and the meiosis-specific kinase Ime2. Genes Dev. 2003; 17:1524–1539. [PubMed: 12783856]

Berchowitz LE, Gajadhar AS, van Werven FJ, De Rosa AA, Samoylova ML, Brar GA, Xu Y, Futcher B, Weissman JS, White FM, et al. A developmentally regulated translational control pathway establishes the meiotic chromosome segregation pattern. Genes Dev. 2013; 27:2147–2163. [PubMed: 24115771]

Bucciantini M, Giannoni E, Chiti F, Baroni F, Formigli L, Zurdo J, Taddei N, Ramponi G, Dobson CM, Stefani M. Inherent toxicity of aggregates implies a common mechanism for protein misfolding diseases. Nature. 2002; 416:507–511. [PubMed: 11932737]

Carlile TM, Amon A. Meiosis I is established through division-specific translational control of a cyclin. Cell. 2008; 133:280–291. [PubMed: 18423199]

Collier B, Gorgoni B, Loveridge C, Cooke HJ, Gray NK. The DAZL family proteins are PABP-binding proteins that regulate translation in germ cells. EMBO J. 2005; 24:2656–2666. [PubMed: 16001084]

Decker CJ, Teixeira D, Parker R. Edc3p and a glutamine/asparagine-rich domain of Lsm4p function in processing body assembly in Saccharomyces cerevisiae. J. Cell Biol. 2007; 179:437–449. [PubMed: 17984320]

DePace AH, Santoso A, Hillner P, Weissman JS. A critical role for amino-terminal glutamine/asparagine repeats in the formation and propagation of a yeast prion. Cell. 1998; 93:1241–1252. [PubMed: 9657156]

Derkatch IL, Liebman SW. Prion-prion interactions. Prion. 2007; 1:161–169. [PubMed: 19164893]

Fowler DM, Koulov AV, Alory-Jost C, Marks MS, Balch WE, Kelly JW. Functional Amyloid Formation within Mammalian Tissue. PLoS Biol. 2005; 4:e6. [PubMed: 16300414]

Haag ES. Rolling back to BOULE. Proc. Natl. Acad. Sci. USA. 2001; 98:6983–6985. [PubMed: 11416173]

Kato M, Han TW, Xie S, Shi K, Du X, Wu LC, Mirzaei H, Goldsmith EJ, Longgood J, Pei J, et al. Cell-free Formation of RNA Granules: Low Complexity Sequence Domains Form Dynamic Fibers within Hydrogels. Cell. 2012; 149:753–767. [PubMed: 22579281]

Kayatekin C, Matlack KES, Hesse WR, Guan Y, Chakrabortee S, Russ J, Wanker EE, Shah JV, Lindquist S. Prion-like proteins sequester and suppress the toxicity of huntingtin exon 1. Proc. Natl. Acad. Sci. 2014; 111:12085–12090. [PubMed: 25092318]

King OD, Gitler AD, Shorter J. The tip of the iceberg: RNA-binding proteins with prion-like domains in neurodegenerative disease. Brain Res. 2012; 1462:61–80. [PubMed: 22445064]

Knowles TPJ, Vendruscolo M, Dobson CM. The amyloid state and its association with protein misfolding diseases. Nat. Rev. Mol. Cell Biol. 2014; 15:384–396. [PubMed: 24854788]

Kronja I, Orr-Weaver TL. Translational regulation of the cell cycle: when, where, how and why? Philos. T. R. Soc. B. 2011; 366:3638–3652.

Li J, McQuade T, Siemer AB, Napetschnig J, Moriwaki K, Hsaio Y, Damko E, Moquin D, Walz T, McDermott A, et al. The RIP1/RIP3 necrosome forms a functional amyloid signaling complex required for programmed necrosis. Cell. 2012; 150:339–350. [PubMed: 22817896]

Loo DT, Copani A, Pike CJ, Whittemore ER, Walencewicz AJ, Cotman CW. Apoptosis is induced by beta-amyloid in cultured central nervous system neurons. Proc. Natl. Acad. Sci. 1993; 90:7951–7955. [PubMed: 8367446]

Maji SK, Perrin MH, Sawaya MR, Jessberger S, Vadodaria K, Rissman RA, Singru PS, Nilsson K, Simon R, Schubert D, et al. Functional amyloids as natural storage of peptide hormones in pituitary secretory granules. Science. 2009; 325:328–332. [PubMed: 19541956]

Majumdar A, Cesario WC, White-Grindley E, Jiang H, Ren F, Khan M, Li L, Choi EM, Kannan K, Guo F, et al. Critical Role of Amyloid-like Oligomers of Drosophila Orb2 in the Persistence of Memory. Cell. 2012; 148:515–529. [PubMed: 22284910]

Miller MP, Unal E, Brar GA, Amon A. Meiosis I chromosome segregation is established through regulation of microtubule-kinetochore interactions. Elife. 2012; 1:e00117. [PubMed: 23275833]

Nilsson MR. Techniques to study amyloid fibril formation in vitro. Methods. 2004; 34:151–160. [PubMed: 15283924]

Reijo R, Lee TY, Salo P, Alagappan R, Brown LG, Rosenberg M, Rozen S, Jaffe T, Straus D, Hovatta O. Diverse spermatogenic defects in humans caused by Y chromosome deletions encompassing a novel RNA-binding protein gene. Nat. Genet. 1995; 10:383–393. [PubMed: 7670487]

Reis Dos S, Coulary-Salin B, Forge V, Lascu I, Bégueret J, Saupe SJ. The HET-s prion protein of the filamentous fungus Podospora anserina aggregates in vitro into amyloid-like fibrils. J. Biol. Chem. 2002; 277:5703–5706. [PubMed: 11733532]

Ruggiu M, Speed R, Taggart M, McKay SJ, Kilanowski F, Saunders P, Dorin J, Cooke HJ. The mouse Dazla gene encodes a cytoplasmic protein essential for gametogenesis. Nature. 1997; 389:73–77. [PubMed: 9288969]

Scherzinger E, Lurz R, Turmaine M, Mangiarini L, Hollenbach B, Hasenbank R, Bates GP, Davies SW, Lehrach H, Wanker EE. Huntingtin-encoded polyglutamine expansions form amyloid-like protein aggregates in vitro and in vivo. Cell. 1997; 90:549–558. [PubMed: 9267034]

Schwartz JC, Wang X, Podell ER, Cech TR. RNA seeds higher-order assembly of FUS protein. Cell Reports. 2013; 5:918–925. [PubMed: 24268778]

Sipe JD, Cohen AS. Review: history of the amyloid fibril. J. Struct. Biol. 2000

Soushko M, Mitchell AP. An RNA-binding protein homologue that promotes sporulation-specific gene expression in Saccharomyces cerevisiae. Yeast. 2000; 16:631–639. [PubMed: 10806425]

Thomas T, Thomas G, McLendon C, Sutton T, Mullan M. β-Amyloid-mediated vasoactivity and vascular endothelial damage. Nature. 1996; 380:168–171. [PubMed: 8600393]

van Werven FJ, Amon A. Regulation of entry into gametogenesis. Philos. T. R. Soc. B. 2011; 366:3521–3531.

Walsh DM, Selkoe DJ. A beta Oligomers - a decade of discovery. J. Neurochem. 2007; 101:1172–1184. [PubMed: 17286590]

Valášek L, Szamecz B, Hinnebusch AG, Nielsen KH. In Vivo Stabilization of Preinitiation Complexes by Formaldehyde Cross-Linking. Method Ezymol. 2007; 429:163–183.

Xu L, Ajimura M, Padmore R, Klein C, Kleckner N. NDT80, a meiosis-specific gene required for exit from pachytene in Saccharomyces cerevisiae. Mol. Cell. Biol. 1995; 15:6572–6581. [PubMed: 8524222]

Article Highlights (85 characters max each)

- Amyloid-like aggregation of the RNA-binding protein Rim4 controls gametogenesis

- The amyloid-like form of Rim4 is active and represses translation

- Aggregation and clearance of Rim4 are developmentally regulated

- Amyloid-like aggregation of RNA-binding proteins during gametogenesis is conserved
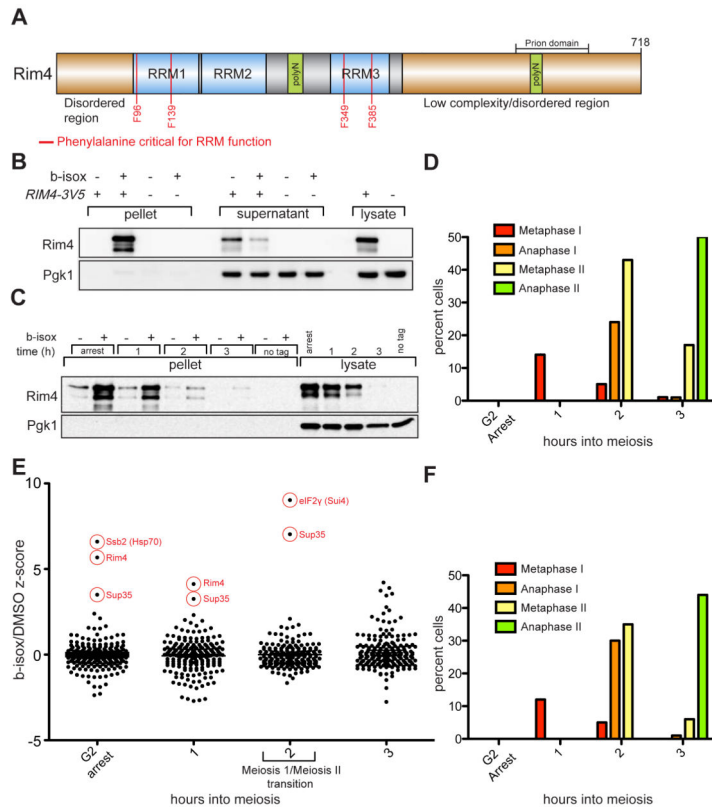
Figure 1.
B-isox binds Rim4 in meiosis I (see **Figure S1** for detailed workflow) **(A)** Diagram of Rim4
(B) *RIM4-3V5*, *pGAL-NDT80*, *GAL4.ER* (A30868) cells were induced to sporulate at 30°C.
After 6 hours when cells had arrested in G 2 due to the lack of Ndt80 lysates were prepared.
Lysates were incubated with 100 μM b-isox (or DMSO control) and Rim4 abundance was
examined by Western blot analysis. Pgk1 did not bind b-isox.

(C) Cells were grown as in (B) except cells were released from the G2 block by the addition
of 1 μM β-estradiol. Lysates were prepared from G2-arrested cells (0 hour) and at 1, 2, and 3
hours post-release and analyzed as in (B).

(D) Meiotic staging data for (C). The percentage of metaphase I, anaphase I, metaphase II,
and anaphase II cells was determined.

(E) *pGAL-NDT80* (A15055) strains carrying the *GAL4.ER* were grown and lysates prepared
as in (C). Precipitated proteins were ITRAQ-labeled and analyzed by mass spectrometry.
Shown are the ratios of b-isox enrichment/DMSO for each identified protein converted to z-
scores.

(F) Meiotic staging data from (E).
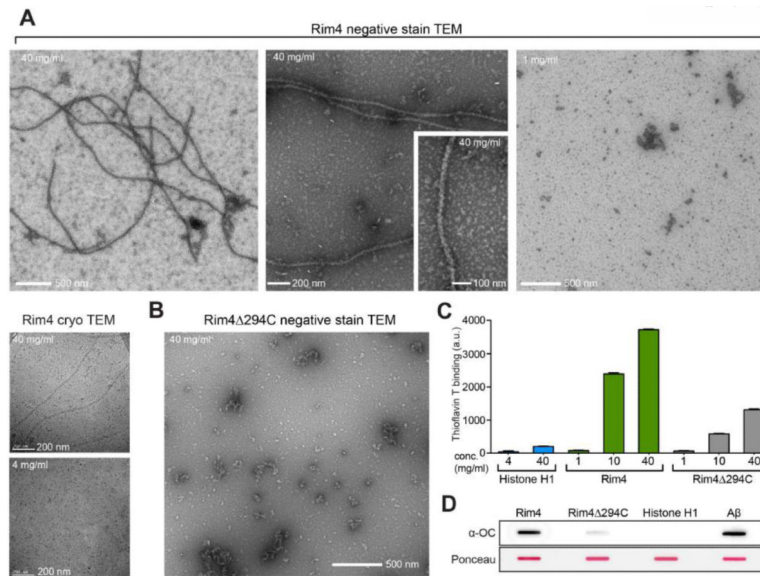
Figure 2.

Rim4 forms amyloid-like aggregates *in vitro*

(A, B) Transmission electron microscopy (TEM) of fibers formed by recombinant Rim4 and Rim4 294C (aa 1-420) incubated at 4°C overnight. The top three panels are micrographs depicting negatively stained samples (prepared at 40 mg/ml and 1 mg/ml). The bottom left panels depict Rim4 samples analyzed by cryo EM at concentrations of 40 mg/ml (left) and 4 mg/ml (right). Scale bars are shown in white.

(C) Recombinant Rim4 and Rim4 294C (various concentrations diluted to 1 mg/ml just before assay) were incubated with 16 ng/ml Thioflavin T, and the fluorescence intensity was measured as in (Nilsson, 2004). Histone H1 at 4 and 40 mg/ml was used as a control.

(D) 10 μg of recombinant protein was slot-blotted onto nitrocellulose and assayed for reactivity with α-amyloid fibril OC. Rim4, Rim4 294C, and Histone H1 concentrated to 40 mg/ml were assayed. Amyloid beta (Aβ, Anaspec) concentrated to 0.25 mg/ml was used as a positive control.
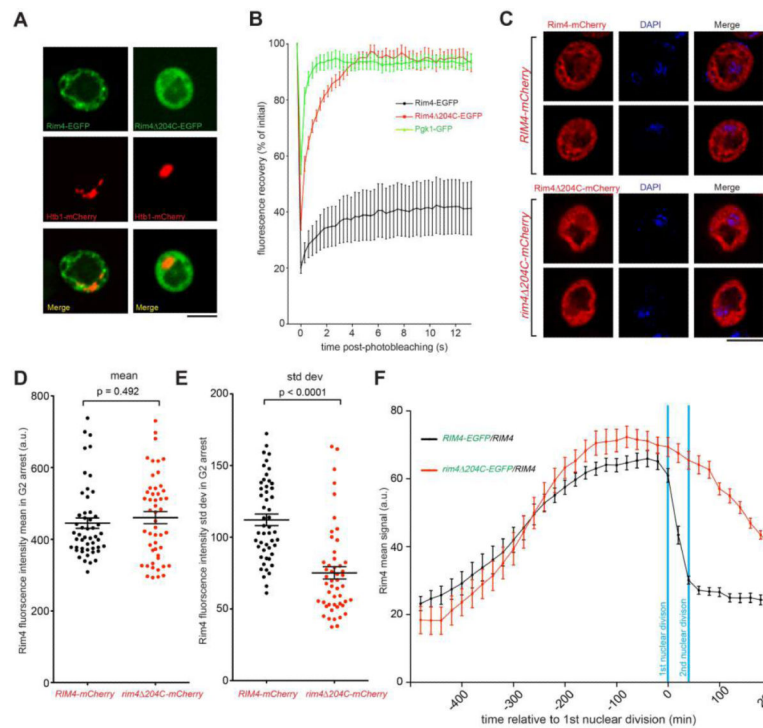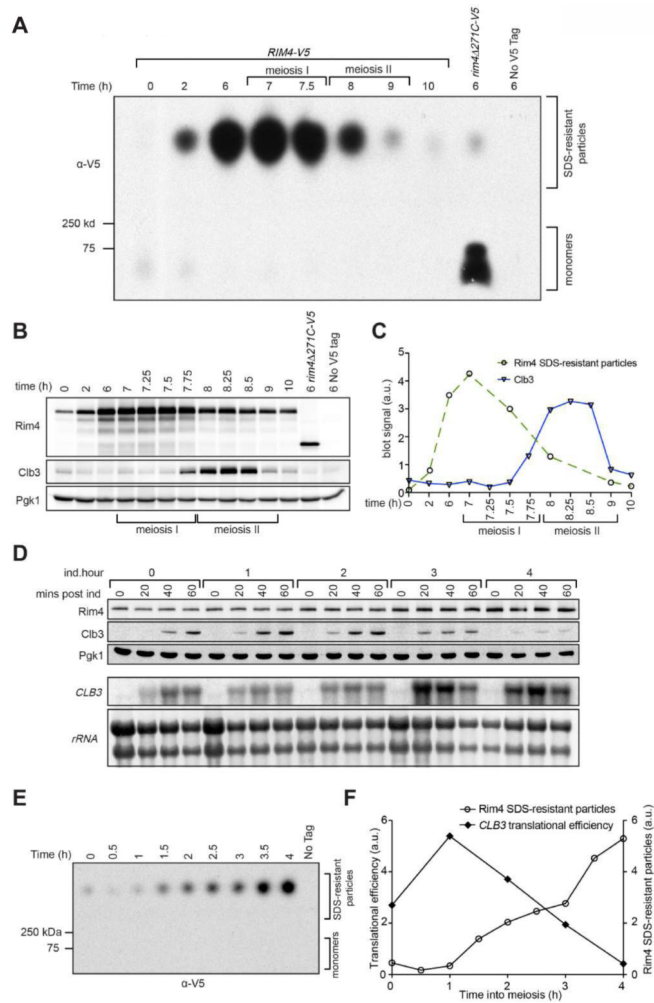
Figure 3.
Evidence that Rim4 forms aggregates in cells

(A, B) Rim4 forms static aggregates in cells. Strains heterozygous for *HTB1-mCherry* and homozygous for either *RIM4-EGFP* (A36245) or *rim4 204C-EGFP* (A36706) were induced to sporulate at 30°C. The mob ility of Rim4 aggregates was determined by FRAP of live cells. Cells were imaged starting at 5 hours after transfer into sporulation medium. A haploid mitotic culture expressing Pgk1-GFP (A34422) was used as a soluble control. Bleached areas were normalized to an unbleached control area. Time point zero was the first observed time point after bleaching. Representative cells are shown in (A) with Rim4 in green and the nucleus in red (scale bar = 5 μm). Signal recovery over time is shown in (B). Plotted is the mean and SEM of 10 cells per strain.

(C-E) *pGAL-NDT80*, *GAL4.ER* cells harboring *RIM4-mCherry* (A35632) or *rim4 204C-mCherry* (A37237) were induced to sporulate at 30°C. After 6 hours when cells had arrested in G2 due to the lack of Ndt80, the cells were fixed and imaged. **(C)** Single-plane images of representative cells arrested in G2 are shown. Scale bar = 5 μm **(D, E)** Rim4-mCherry signal (vacuole excluded) was quantified in the central z-plane. The mean Rim4 signal is not significantly different between the two strains however the standard deviation (aggregation proxy) is significantly different. n = 50 cells per strain.

(F) Cells either harboring a *RIM4-EGFP* (A36775) or *rim4 204C-EGFP* (A36773) fusion were induced to sporulate at 30°C. After 1 h our of growth in batch culture, the cells were loaded onto a microfluidics chip and imaged every 20 minutes. See also Figures S3A-C and **Movies S3-S6**. A quantification of Rim4-EGFP signal over time is shown. Plots were aligned according to the first meiotic division. Cells harboring *RIM4-EGFP* and *rim4 204C-EGFP* are shown in black and red, respectively. Plotted is the mean and SEM of 10 cells per strain. Scale bar = 5 μm

Figure 4.

Rim4 forms amyloid-like aggregates *in vivo* to repress translation

(A) Rim4 amyloid-like aggregates form during premeiotic S phase which are cleared during meiosis II. *pGAL-NDT80* cells (A30868) were induced to sporulate and Rim4's ability to form SDS-resistant aggregates was analyzed as in (Alberti et al., 2009). Samples were incubated in 2% SDS for 10 min and resolved on 1.7% agarose (with 0.1% SDS) and Rim4 was detected by immunoblot analysis. A strain harboring Rim4 lacking its C-terminal LC sequences (A33848) is shown as a control.

(B, C) Western blot analysis of time course shown in 4A. Total levels of Rim4-3V5, Clb3-3HA, and Pgk1 (loading control) are shown in (B). Quantification of blots is shown in (C). Rim4 SDS-resistant aggregates were quantified from SDD-AGE in Figure 4A and Clb3 from SDS-PAGE in Figure 4B. Total levels of Rim4 and Clb3 were normalized to Pgk1.

(D-F) *CLB3* translational repression begins between 2 and 3 hours after induction of sporulation (see **Figure S4A** for detailed workflow). A culture harboring *RIM-3V5*, *GAL4.ER*, and *pGAL-5′UTR$_{CLB3}$-CLB3* (A35430) was split and induced to sporulate at 30°C. *pGAL-5′UTR$_{CLB3}$-CLB3* was induced by β-estradiol at the indicated time. Rim4-3V5, Clb3-3HA, and Pgk1 (loading control) protein and *CLB3* mRNA and *rRNA* (loading control)
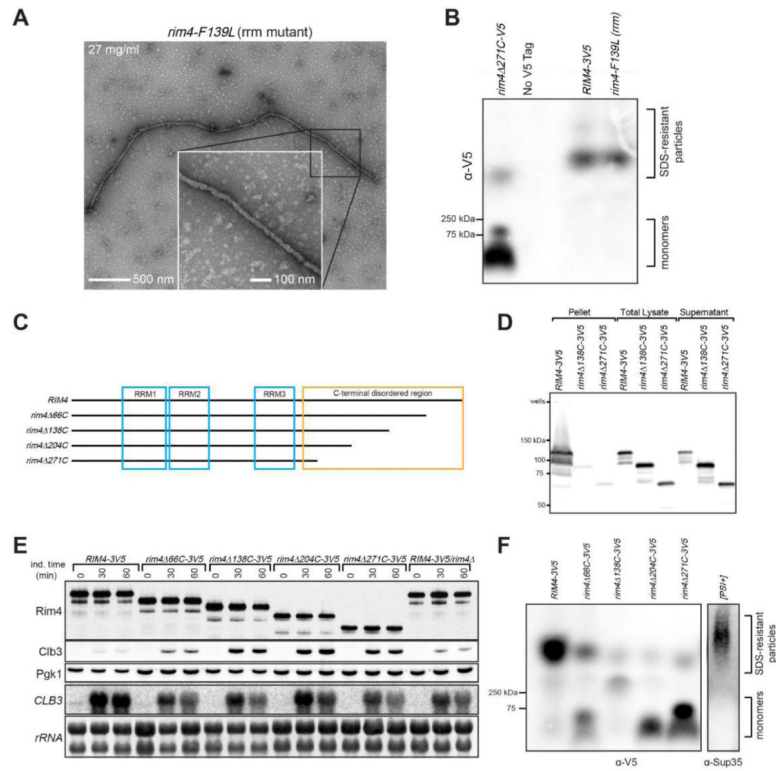
levels were determined at the indicated times following β-estradiol addition (D). SDS-resistant Rim4 aggregates were analyzed in (E). A quantification of Rim4 aggregate formation (open circles) and Clb3 translation (Clb3 protein/*CLB3* mRNA after 60 min induction: closed circles) is shown in (F).

Figure 5.
The LC sequences, but not RNA-binding are required for Rim4 aggregation

(A) TEM of fibers formed by Rim4-F139L (RRM mutant) concentrated to 27 mg/ml and incubated at 4°C overnight.

(B) RNA binding is not required for amyloid-like aggregation. Rim4 was analyzed by SDD-AGE six hours after transfer into sporulation-inducing conditions of cells harboring *rim4 271C-3V5* (A35408), a no-tag control (A15055), *RIM4-3V5* (A35430), and *rim4-F139L-3V5* (rrm mutant A35324).

(C) Diagram of Rim4 C-terminal truncations

(D) Rim4 can be pelleted from detergent-containing undenatured lysate. Strains harboring *RIM4-3V5* (A35430), *rim4 138C-3V5* (A35402), and *rim4 271C-3V5* (A35408) were arrested in G2 as above. Native lysates were prepared and spun for 60 min at 250,000*g*. Rim4 levels were determined in total lysate, pellet and supernatant.

(E, F) *rim4* mutants that fail to form amyloid-like aggregates are defective for translational control. Strains harboring *RIM4-3V5* (A35430), heterozygous *RIM4-3V5/rim4?* (A35841) and constructs shown in (C) (A35399, A35402, A35405, A35408) as well as *pGAL-5′UTR$_{CLB3}$-CLB3, ndt80?*, *ZIP1-GFP*, *SPC42-mCherry*, and *GAL4.ER* were arrested in G2 (6 hours) and *pGAL-5′UTR$_{CLB3}$-CLB3* was induced by β-estradiol addition. Rim4-3V5, Clb3-3HA, and Pgk1 (loading control) protein and *CLB3* mRNA and *rRNA* (loading control) were determined (E). SDS-resistant Rim4 aggregates (at 6 hours) were analyzed in (F). The Sup35 aggregate-forming strain ([*PSI+*]; A25208) was used as a positive control.
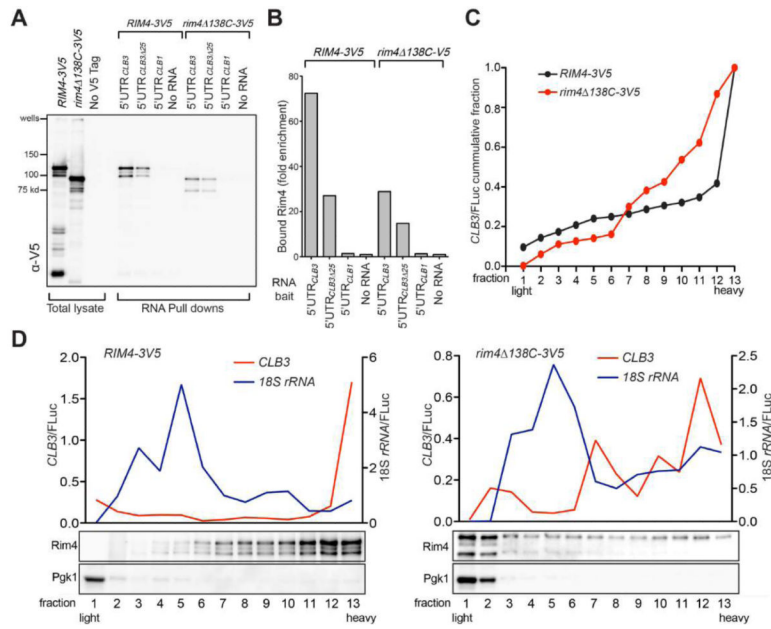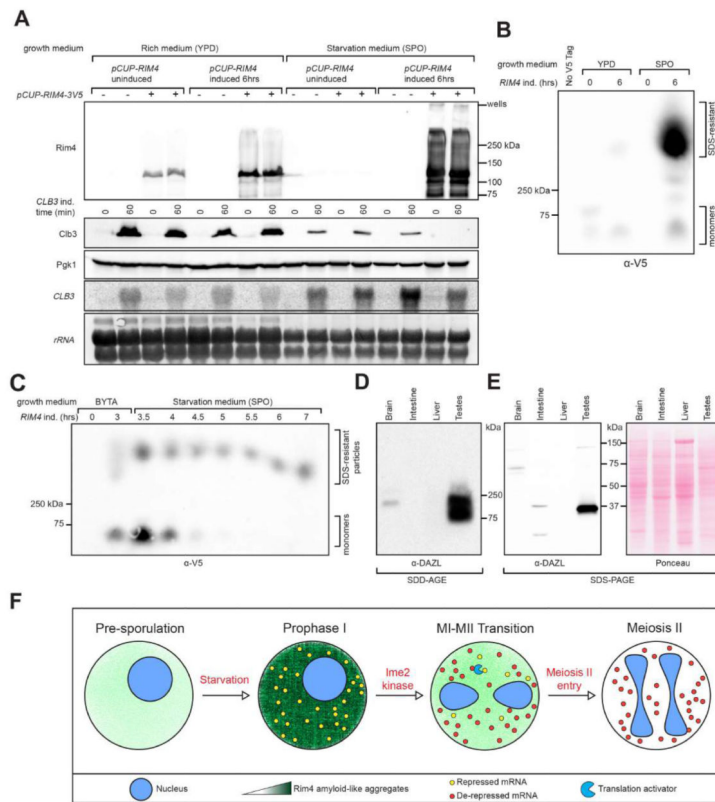
Figure 6.
Effects of the LC sequences on Rim4 RNA binding and *CLB3* mRNA mobility in sucrose gradients

(A, B) An aggregation-defective *rim4* mutant has decreased RNA-binding activity. Extracts from *RIM4-3V5* (A35430) and *rim4 138C-3V5* (A35402) cells arrested in G2 (6 hours) were incubated with *in vitro* transcribed 3′ biotinylated RNAs conjugated to streptavidin magnetic beads. Beads were recovered and boiled in SDS loading buffer to release bound factors. Shown is the amount of Rim4 recovered using the indicated RNA baits (A). Quantifications (B) were input-normalized and are shown as fold enrichment over the no-RNA control.

(**C, D**) Rim4 and its bound mRNA targets exist in heavy mRNPs. Strains harboring *RIM4-3V5* (A35430) and *rim4 138C-3V5* (A35402) were arrested in G2 as above except *CLB3* was expressed by the addition of β-estradiol for 60 minutes prior to collection. Samples were fixed in 1% formaldehyde on ice for 15 mins (stopped by the addition of 0.1 M glycine) to preserve the RNPs (Valazek et al., 2007). Native lysates were fractionated on 10-50% sucrose gradients. Sedimentaton of Rim4, Pgk1 as well as *CLB3* mRNA and 18S rRNA was determined by immunoblot and qPCR, respectively. RNA quantification was normalized to luciferase RNA which was spiked into each fraction in equal amounts to normalize for RNA extraction efficiency.

Figure 7.
Formation of Rim4 amyloid-like aggregates is regulated by starvation (**A, B**) Starvation triggers Rim4 aggregation and translational repression (for detailed workflow see **Figure S6A**). Haploid *GAL4.ER*, *pGAL-5′UTR_{CLB3}-CLB3* strains with or without *pCUP1-RIM4-3V5* (A34980, A28492) were diluted to $OD_{600} = 1.8$ in either YEPD or SPO medium. *pCUP1-RIM4* was induced by the addition of 25 μm $CuSO_4$. *pGAL-5′UTR_{CLB3}-CLB3* was induced by 2 μM β-estradiol prior to (0 hr) and after (6 hr) $CuSO_4$ induction for 60 minutes. Rim4-3V5, Clb3-3HA, and Pgk1 (loading control) protein and *CLB3* mRNA and *rRNA* (loading control) levels were determined at the indicated times in (A). SDS-resistant Rim4 aggregates (prior to and after $CuSO_4$ induction) were analyzed by SDD-AGE in (B).
(**C**) Monomeric Rim4 is converted into amyloid-like aggregates upon starvation (for detailed workflow see **Figure S6B**). A haploid *pGAL-RIM4-3V5* strain was grown in BYTA medium in the presence of 1 μM β-estradiol for 3 hours to induce Rim4 expression. Cells were then shifted to SPO medium. Rim4 SDS-resistant aggregates were assayed. Rim4 and Pgk1 protein levels from TCA extracts were analyzed in (**Figure S6C**).
(**D, E**) DAZL forms SDS-resistant aggregates in mouse gametogenesis. Brain, intestine, liver, and testes were harvested from a 2 month old C57BL/6J male mouse. Samples were Dounce homogenized in SDD-AGE buffer and analyzed by SDD-AGE (D) and SDS-PAGE (E) DAZL was detected by immunoblot analysis.
(**F**) Model for Rim4-mediated translational control. See text for details.